GLIA

WILEY

RESEARCH ARTICLE

Adenosine A$_{2B}$ receptors differently modulate oligodendrogliogenesis and myelination depending on their cellular localization

Federica Cherchi[1] | Martina Venturini[1] | Giada Magni[2] | Lucia Frulloni[1] |
Martina Chieca[3] | Daniela Buonvicino[3] | Clara Santalmasi[1] |
Francesca Rossi[2] | Francesco De Logu[3] | Elisabetta Coppi[1] |
Anna Maria Pugliese[1]

[1]Department of Neuroscience, Psychology, Drug Research and Child Health (NEUROFARBA), University of Florence, Florence, Italy

[2]Cnr—Istituto di Fisica Applicata "Nello Carrara", Florence, Italy

[3]Department of Health Sciences, Section of Clinical Pharmacology and Oncology, University of Florence, Florence, Italy

Correspondence
Federica Cherchi, Department of Neuroscience, Psychology, Drug Research and Child Health (NEUROFARBA), University of Florence, Florence 50139, Italy.
Email: federica.cherchi@unifi.it

Abstract

Differentiation of oligodendrocyte precursor cells (OPCs) into mature oligodendrocytes (OLs) is a key event for axonal myelination in the brain; this process fails during demyelinating pathologies. Adenosine is emerging as an important player in oligodendrogliogenesis, by activating its metabotropic receptors (A$_1$R, A$_{2A}$R, A$_{2B}$R, and A$_3$R). We previously demonstrated that the Gs-coupled A$_{2B}$R reduced differentiation of primary OPC cultures by inhibiting delayed rectifier (I$_K$) as well as transient (I$_A$) outward K$^+$ currents. To deepen the unclear role of this receptor subtype in neuron-OL interplay and in myelination process, we tested the effects of different A$_{2B}$R ligands in a dorsal root ganglion neuron (DRGN)/OPC cocultures, a corroborated in vitro myelination assay. The A$_{2B}$R agonist, BAY60-6583, significantly reduced myelin basic protein levels but simultaneously increased myelination index in DRGN/OPC cocultures analyzed by confocal microscopy. The last effect was prevented by the selective A$_{2B}$R antagonists, PSB-603 and MRS1706. To clarify this unexpected data, we wondered whether A$_{2B}$Rs could play a functional role on DRGNs. We first demonstrated, by immunocytochemistry, that primary DRGN monoculture expressed A$_{2B}$Rs. Their selective activation by BAY60-6583 enhanced DRGN excitability, as demonstrated by increased action potential firing, decreased rheobase and depolarized resting membrane potential and were prevented by PSB-603. Throughout this A$_{2B}$R-dependent enhancement of neuronal activity, DRGNs could release factors to facilitate myelination processes. Finally, silencing A$_{2B}$R in DRGNs alone prevents the increased myelination induced by BAY60-6583 in cocultures. In conclusion, our data suggest a different role of A$_{2B}$R during oligodendrogliogenesis and myelination, depending on their activation on neurons or oligodendroglial cells.

Martina Venturini and Giada Magni contributed equally for this work.

1 | INTRODUCTION

Oligodendrocytes (OLs) are the cells responsible for myelin production in the central nervous system (CNS). Rapid communication between neurons requires myelin enwrapping of nerve fibers to allow saltatory propagation of electrical impulses (Cohen et al., 2020). In addition, OLs promote neuronal metabolism, and stabilize axonal cytoskeleton (Meyer et al., 2018; Philips & Rothstein, 2017). Differentiation of OL precursor cells (OPCs) into mature OLs is a key event for axonal myelination in the brain; this process fails during demyelinating pathologies, such as multiple sclerosis (Tepavčević & Lubetzki, 2022). Pre-OLs lose their bipolarity when they interact with a target axon, developing a ramified shape and beginning to produce filamentous myelin outgrowths (Kuhn et al., 2019). It was demonstrated that OPCs receive synaptic inputs from neurons (Bergles et al., 2000; De Biase et al., 2010; Kukley et al., 2010; Sun et al., 2016) and express neurotransmitter receptors, including those for glutamate (Bergles et al., 2000; Gallo et al., 2008; Krasnow & Attwell, 2016), indicating a physiological interaction between OLs and neurons. It is no wonder that neuronal activity is a key event for white matter development (Forbes & Gallo, 2017) as well for myelin thickness or internode length rearrangement during synaptic plasticity (Suminaite et al., 2019). In the last years different mechanisms have been suggested by which neuronal activity controls OPC migration, proliferation, differentiation, or survival (Arellano et al., 2016; Barres & Raff, 1993, 1999; Duncan et al., 2021; Saab et al., 2016; Simons & Nave, 2015). In the CNS, it has been demonstrated that myelination may be regulated, among others, by the activity of the nearby neurons (Lundgaard et al., 2013). In particular, axon-dependent myelination is a key event for myelin remodeling, as well as for remyelination processes in the adult, since both are reduced by N-methyl-D-aspartate (NMDA) blockers (Li et al., 2013; Lundgaard et al., 2013). However, the role of NMDA it is still under debate, as evidence also indicated that AMPA receptors prevail in modulating oligodendrogliogenesis and myelination (De Biase et al., 2011; Fannon et al., 2015; Krasnow & Attwell, 2016; Zonouzi et al., 2011). Several factors, beyond glutamate and its receptors, control the interplay between neurons and OLs. For example, action potential (AP)-dependent release of growth factors or GABA could modulate OPC proliferation, as well as axon myelination (Barres & Raff, 1993; Cherchi, Bulli, et al., 2021; Marinelli et al., 2016).

Among the many oligodendrogliogenesis modulators, there is adenosine and its metabotropic receptors (A$_1$R, A$_{2A}$R, A$_{2B}$R, and A$_3$R). The A$_1$R and A$_3$R are coupled to G$_{i/o}$ proteins while A$_{2A}$R and A$_{2B}$R are coupled to G$_{s/olf}$ proteins (Fredholm et al., 2011); however, A$_1$R, A$_3$R, and A$_{2B}$R can also activate phospholipase C through G$_q$ protein (Antonioli et al., 2013). All adenosine receptors are expressed during the whole process of OPC maturation and exert a key role in oligodendrogliogenesis (Cherchi, Pugliese, & Coppi, 2021; Fields, 2004;

Stevens et al., 2002). In 2002 Stevens and collaborators demonstrated that adenosine is a potent axonal-dependent signal promoting OPC differentiation and myelination (Stevens et al., 2002). However, they might underestimate the role of A$_{2B}$R, probably because of the paucity of selective ligands (Popoli & Pepponi, 2012). Of note, A$_{2B}$R presents the lowest affinity for adenosine among the other receptors, that is in the micromolar respect to nanomolar ranges (Pedata et al., 2016). The high adenosine concentrations, that is 30–50 μM during cerebral ischemia (Latini & Pedata, 2001), are reached under pathological conditions, indicating A$_{2B}$R as important therapeutic target (Coppi, Dettori, et al., 2020; Pedata et al., 2016). Different in vivo models of demyelination link A$_{2B}$R activation to a more severe symptomatology. In particular, Wei and collaborators first observed an upregulation of A$_{2B}$R in peripheral blood leukocytes of multiple sclerosis patients, as well as in peripheral lymphoid tissues of experimental autoimmune encephalomyelitis (EAE) mice (Wei et al., 2013). Moreover, they demonstrate that either blockade or deletion of A$_{2B}$R leads to a less severe EAE, by reducing adenosine-mediated Th17 lymphocyte differentiation and interleukin-6 (IL-6) release (Wei et al., 2013). Accordingly, in an animal model of sensorineural hearing loss (SNHL) the block of A$_{2B}$R improves never fiber density and myelin compaction in the auditory nerve (Manalo et al., 2020). On the other hand, this article describes a protective effect of A$_{2B}$R stimulation in a demyelinating mouse model of schizophrenia induced by the NMDA antagonist MK-801 (Ma et al., 2022), indicating an enigmatic role of A$_{2B}$R in these processes.

Our previous work demonstrated that the G$_s$-coupled A$_{2B}$R delays in vitro OPC maturation by inhibiting potassium delayed rectifier outward currents (I$_K$) as well as transient outward K$^+$ (I$_A$) currents (Coppi, Cherchi, et al., 2020). Both these currents are prominent in OPCs, and it is well described their involvement in oligodendrogliogenesis as their inhibition by pharmacological or genetic tools decreases OPC differentiation and myelin production (Attali et al., 1997; Cherchi, Bulli, et al., 2021; Chittajallu et al., 2002, 2004; Coppi et al., 2013; Vautier et al., 2004). In addition, the A$_{2B}$R-mediated effect on K$^+$ currents was mediated by intracellular cyclic AMP (cAMP) rise, consistent with G$_s$ protein activation (Coppi, Cherchi, et al., 2020). Nevertheless, A$_{2B}$Rs are also expressed by neuronal cells (Christofi et al., 2001; Corset et al., 2000; Gonçalves et al., 2015) and it is well described that this receptor increases glutamate release in hippocampal CA1 presynaptic terminals (Fusco et al., 2019; Gonçalves et al., 2015). In addition, A$_{2B}$Rs are implicated in mediating netrin-1-dependent axon outgrowth, indicating another functional role of A$_{2B}$Rs in CNS beyond their known activity in neurotransmission (Corset et al., 2000). Recently, it was also demonstrated that A$_{2B}$Rs promote axon regeneration and survival both in *Drosophila* C3da and mice retinal neurons through stimulation of neuronal activity and gliotransmission (Wang et al., 2023).

On these bases, the role of A_{2B}Rs in neuron-OLs interplay appears unclear. To investigate this complex scenario we first studied the role of A_{2B}R in an in vitro model of dorsal root ganglion neurons (DRGNs) cocultured with OPCs. We confirm that the selective stimulation of A_{2B}Rs reduces OPCs differentiation, in accord with our previous findings (Coppi, Cherchi, et al., 2020), but unexpectedly it increases axon myelination. We also found that rat DRGNs express functional A_{2B}Rs and their stimulation increases neuronal activity, an effect that might promote axon myelination. Moreover, downregulation of this receptor subtype selectively in DRGNs prevents the increase in myelination index, but not the reduction in OPC differentiation, mediated by BAY60-6583. Our data suggest a different role of A_{2B}Rs during oligodendrogliogenesis and myelination, depending on their cellular localization. We hypothesize that A_{2B}R localized on OPCs negatively modulates cell maturation, while the same receptor expressed on DRGNs, by increasing AP firing, seems to promote OPC recruitment and myelination of active axons.

2 | METHODS

2.1 | Animals

Wistar rats (Envigo, Italy) were used for the preparation of primary cultures of DRGNs and mixed glial cells. All animal experiments satisfied the regulatory requirements of the European Parliament (Directive 2010/63/EU), European Union Council (September 22, 2010), and Italian Animal Welfare Law (DL 26/2014). The protocol received approval from the Institutional Animal Care and Use Committee (Univ. Florence) and the Italian Ministry of Health. Animal suffering and the animal number required for data reproducibility were minimized, accordingly with the Ministerial notification (ser. no. 211/2022).

2.2 | Cell culture preparation

2.2.1 | DRGN cultures

For electrophysiological recordings, DRGNs were prepared from 3 to 4 weeks old rats as described (Coppi et al., 2019). For OPC/DRGN cocultures, DRGs were isolated from P5-6 pups. Briefly, ganglia were bilaterally removed and dissociated with 2 mg/mL of type 1A collagenase (Merck, Germany, #C9891) and 1 mg/mL of trypsin (Merck, Germany, #T9201) in Hank's balanced salt solution (Merck, Germany, #H8264) at 37°C for 30 min. Cells were then pelleted and subjected to mechanical digestion. After, the cells were centrifuged and suspended in Dulbecco's Modified Eagle's Medium (DMEM; Euroclone, Italy, #ECB750) supplemented with 100 U/mL penicillin/streptomycin (P/S; Merck, Germany, #P0781), 4 mM L-glutamine (L-Gln; Merck, Germany, #59202C), and 20% fetal bovine serum (FBS; Merck, Germany, #F7524), nerve growth factor (NGF, 100 ng/mL; Thermo Fisher, USA, # A42578) was added to promote neuron

survival, while cytosine arabinoside (Ara-C, 10 mM; Merck, Germany, #C1768) was supplemented to remove eventual contaminating fibroblasts and glial cells. DRGNs were then plated on 13-mm glass coverslip (10,000 cells/well) coated by 8.3 mM poly-L-lysine (Merck, Germany, #P4832) and 5 mM laminin (Merck, Germany, #L2020). Cells were cultured for 1–2 days before being used for patch-clamp experiments. For OPC/DRGN cocultures, DRGNs were suspended in Neurobasal medium (NB; Thermo Fisher, USA, #21103049) supplemented with 2% B27 (Thermo Fisher, USA, #17504044), 100 U/mL P/S and 4 mM L-Gln and plated at a density of 15,000 cells per well. Following isolation, DRGNs were maintained in NB medium to permit neurite out-growth for at least 1 weeks prior to seeding with OPC. Two days before seeding OPCs onto DRGN culture, Ara-C was removed.

2.2.2 | OPC cultures

OPCs were prepared from P1 to P2 rats, as described (Coppi, Cherchi, et al., 2020). Briefly, rat pups were sacrificed, and cortices removed, mechanically and enzymatically dissociated, suspended in DMEM containing 20% FBS, 100 U/mL P/S, and 4 mM L-Gln, and plated in poly-L-lysin coated T75 flasks. After 7 days in culture, microglial cells were removed from the mixed glial cells by a 1 h preshake. OPCs were then separated from glial cultures by 5 h of horizontal shaking. Suspended separated cells were then replated onto plastic culture dishes for an additional 30 min, to allow adhesion of residual microglial cells. During the last phase of OPC preparation (shaking), NGF was removed from DRGN cultures since it was demonstrated to reduce OPC differentiation (Chan et al., 2004; Lee et al., 2007; Vaes et al., 2021).

2.2.3 | DRGN/OPC cocultures

Purified OPCs were then suspended in the same NB medium described above and seeded onto DRGNs at a density of 50,000 cells per well. OPC/DRGN cocultures were maintained for a maximum of 21 days in the presence of the pro-myelinating hormone T3 (50 nM; Merck, Germany, #T6397) (Calza et al., 2002). In order to study the effect of A_{2B}R on myelination processes, selective ligands for this receptor subtype were added every 2 days from t_3 to t_{14}, considering the time 0 (t_0) as the day at which OPCs were added onto DRGNs.

2.3 | Patch-clamp recordings

Whole-cell patch-clamp recordings have been performed on DRGNs isolated from 3 to 4 weeks old rats. To this purpose, cells were transferred to a recording chamber (1 mL volume) mounted on the platform of an inverted microscope (Olympus CKX41, Milan, Italy) and superfused at a flow rate of 1.5 mL/min with a standard K^+-containing extracellular solution (mM): NaCl 147; KCl 4; $MgCl_2$ 1; $CaCl_2$ 2; HEPES (4-(2-hydroxyethyl)-1-piperazineethanesulfonic acid) 10; and

D-glucose 10 (pH 7.4 with NaOH). Borosilicate glass electrodes (Harvard Apparatus, Holliston, Massachusetts USA) were pulled with a Sutter Instruments puller (model P-87) to a final tip resistance suitable for cell investigated (5 MΩ). The electrode was filled with standard K$^+$-based pipette solution (mM): K-gluconate 130; NaCl 4.8; KCl 10; MgCl$_2$ 2; CaCl$_2$ 1; Na$_2$-ATP 2; Na$_2$-GTP 0.3; EGTA 3; and HEPES 10 (pH 7.4 with KOH). Then, data were acquired with an Axopatch 200B amplifier (Axon Instruments, CA, USA), low pass filtered at 10 kHz, stored, and analyzed with pClamp 9.2 software (Axon Instruments, CA, USA). All the experiments were carried out at room temperature (RT: 20–22°C). All drugs were dissolved in extracellular solution and were applied by superfusion with a three-way perfusion valve controller (Harvard Apparatus, Holliston, MA, USA) after a stable baseline was obtained. A complete exchange of bath solution in the recording chamber was achieved within 28 s. Whole-cell patch-clamp recordings were performed on small-medium sized (Cm < 25 pF) DRGNs (averaged Cm was 19.9 pF in 30 cells investigated).

For measuring the rheobase, the minimum current that elicits an AP, a series of current steps (1200 ms) was injected, from -10 pA with increments of 10 pA, until the AP firing accommodates, before and after drug application. With this protocol, also input resistance was measured, from the -10 pA step. To monitor the trend of resting membrane potential (RMP) and the frequency of APs over time, a protocol consisting of a depolarizing step of 10 pA and lasting 10 ms, repeated every 15 s, was also applied. From the third AP of three depolarizing step, before and after drug application, the following AP parameters was measured: amplitude, calculated as the difference between the peak reached by the overshoot and the threshold; half-width as the time to reach half AP amplitude (ms); upstroke and downstroke phase as the maximum value of the rising slope (dV/dt) and the maximum decay slope (dV/dt), respectively. Current-clamp recordings were filtered at 10 kHz and digitized at 1 kHz.

2.4 | Constructs

Construct pAAV-CMV-EGFP expressing rat *Adora2b* (rA$_{2B}$) short hairpin RNA (shRNA) was obtained using the following: shRNA sequence 5′-CCATGAGCTACATGGTTTATTT-3′ according to RNAi Consortium of Broad Institute libraries. pAAV-CMV-EGFP-ratA$_{2B}$[mir30-shRNA] was generated with PCR amplification of a donor plasmid using two oligonucleotides (FW 5′-ACAGATGTAAAATAAACCATGTAGCTCATG Gtgcctactgcctcggacttcaag-3′ and REV: 5′-GGCTTCACTAAAATAAA CCATGTAGCTCATGTcgctcactgtcaacagcaatatacct-3′). After purification, PCR product was phosphorylated with T4 PNK (NEB, #M0201S) and ligated and circularized with T4 ligase (Thermo Fisher #K1423). shRNA expressing plasmid was validated with Sanger sequencing.

2.5 | AAV generation and DRGNs infection

Recombinant Adeno associated virus (rAAV) was generated as previously reported (Landini et al., 2023). Briefly, AAVpro HEK293 cells (#632273, Takara, RRID:CVCL_B0XW) were triple transfected using PEI (#23966, Polyscience) in a 1:3 ratio of DNA:PEI with pAAV-CMV-EGFP-ratA$_{2B}$[mir30-shRNA], pAdDeltaF6; (#112867, Addgene) and pAAV Rep/Cap 2/5 (#104964 Addgene), 1:1:1 molar ratio. Seventy-two hours posttransfection, rAAVs virions were collected, purified with ultracentrifugation through an iodixanol gradient, concentrated with Amicon Ultra-15 centrifugal filter units (molecular weight cutoff, 100 kDa; Merck Millipore) and quantified as 2×10^{10} gc/μL using RT-qPCR assay (#6233 AAVpro Titration Kit, Takara). Two days after DRGNs plating, rAAV was added in the culture medium (20 μL/well) and was maintained for 72 h. Thereafter, medium containing AAV was removed and fresh medium was added for 2 days, before adding OPCs.

2.6 | Quantitative RT-PCR analysis

Total RNA was isolated using Trizol Reagent (Life Technologies, Monza, Italy). One μg of RNA was retrotranscribed using iScript (Bio-Rad, Milan, Italy). RT-qPCR was performed as reported (Buonvicino et al., 2018). The following primers were used for: MAG: forward 5′-AACTACCCGCCAGTGGTCTTCAAGTC-3′ and reverse 5′-ACGCTG TGCTCCGAGAAGGTGTAC-3′; MBP: FW: 5′-CCATCCAAGAAGAT CCCACAGCAGC-3′ and RV: 5′-GCGCACCCCTGTCACCGCTAAA-3′; Beta-actin: FW: 5′-TCCCTGTATGCCTCTGGTCGTACC-3′ and RV: 5′-TCCCTCTCAGCTGTGGTGGTGAAG-3′; A$_{2B}$: FW: 5′- GTGGGAGC CTCGAGTGCTTTACAG $-3′$ and RV: 5′-GCCAAGAGGCTAAAGATG GAGCTCTG-3′. Primers were purchased from Integrated DNA Technologies (Iowa, USA).

2.7 | Immunocytochemistry

DRGNs cultures and OPC/DRGN cocultures were fixed with 4% paraformaldehyde in 0.1 M phosphate-buffered saline (PBS, Corning, USA, #21-030-CV) for 10 min at RT. Cells were washed twice with PBS and then incubated in PBS solution containing 0.25% Triton X-100 (PBST; Merck, Germany, #X100). After three washes in PBS, cells were incubated in blocking buffer (BB, 10% normal goat serum (GS; Merck, Germany, #G9023) in PBST) for 30 min to block unspecific binding sites. Cells were then incubated for 2.5 h at RT with the appropriate primary antibodies, dissolved in BB. Finally, cells were washed three times with PBS and then incubated 1 h at RT with specific secondary antibodies dissolved in BB. Coverslips were mounted with Fluoroshield (Merck, Germany, #F6057) containing 4′,6-diamidino- 2-phenylindole (DAPI) to stain cell nuclei. For primary DRGN cultures the following primary antibodies were used: mouse anti-βIII-Tubulin (1:200; Invitrogen, USA, #MA1-118X) and rabbit anti-A$_{2B}$R (1:200; Alomone, Israel, #AAR-003; Chemicon, USA, #AB1589P). For OPC/DRGN coculture: rabbit anti-βIII-Tubulin (1:400; Cell Signaling, USA, #D71G9) and mouse anti-myelin basic protein (MBP) (1:500; Cell Signaling, USA, #E9P7U). AlexaFluor 488 donkey anti-rabbit (1:500; Invitrogen, USA,

#A21206) and AlexaFluor 555 donkey anti-mouse (1:500; Invitrogen, USA, #A31570) were used as fluorescent secondary antibodies. Coverslip were mounted with Fluoroshield containing DAPI to stain cell nuclei. Concerning those experiments in which DRGNs have been infected with AAV expressing shA$_{2B}$R and GFP, GS was replaced by 10% donkey serum (DS; Merck, Germany, #S30). Cells were then incubated for 1.5 h at RT with the goat anti-GFP (1:2000; Abcam, UK, #ab5450) dissolved in BB and washed three times with PBS. Samples were incubated 1 h at RT with 488 donkey anti-goat (1:500; Abcam, UK, #ab150129), washed three times with PBS and incubated 2.5 h with the primary antibodies mentioned above. After three washes with PBS, cells are incubated with 555 goat anti-rabbit (1:500; Abcam, UK, #ab150078) and 647 goat anti-mouse (1:500; Abcam, UK, #ab150115). Coverslip were mounted with Fluoroshield containing DAPI to stain cell nuclei. Control experiments were performed by incubating fixed cells only with the secondary antibodies and DAPI to exclude nonspecific signals.

2.8 | Confocal microscopy and quantitative analysis

Immunocytochemical images were captured by a Leica SP8 laser scanning confocal microscope (Leica Microsystems, Mannheim, Germany). In order to visualize A$_{2B}$R expression on DRGNs, a $63\times/1.40$ oil-immersed objective was used and the following parameters of acquisition were applied: 2048×2048 pixels format, scanning speed 200 Hz, z-step 0.5 μm. OPC/DRGN coculture images were acquired with a $20\times/0.40$ objective using the following capture setting: 2048×2048 pixels, scanning speed of acquisition 200 Hz and z-step of 1 μm. The collected OPC/DRGN images were acquired blind and were analyzed by a different researcher with an open-source software (Fiji-ImageJ, version 1.49v National Institutes of Health, Bethesda, MD, USA; Schneider et al., 2012). MBP immunofluorescence was quantified by the number of positive pixels above a threshold level in each confocal microscopy z-projection of 10 consecutive confocal z-scans (total thickness 10 μm; Gerace et al., 2021) with the threshold tool in 3 random fields per coverslip. In the same images, the Manders' overlap coefficient (M1) was also evaluated: this parameter represents the myelination index, estimated as the fraction of βIII-Tubulin positive pixels overlapping the MBP positive pixels in each region of interest (ROI), by using JACop plugin of ImageJ (Bolte & Cordelières, 2006; Igado et al., 2020). The number of cocultures was represented by the symbol "N," while the number of replications of every single condition was indicated by the lowercase letter "n." Sholl ramification analysis was performed for MBP$^+$ cells that were segmented and transformed into a binary mask before tracing the cellular processes by using Simple Neurite Tracer tool (Gensel et al., 2010). Total length of the oligodendrocyte ramifications and the number of primary branches were measured. Concentric circles were placed around the traced cell starting from the soma and radiating outward at increasing radial increments of

5 μm. The number of intersections was enumerated as points where cellular processes of each cell cross a concentric Sholl ring. The number of intersections per circle was also plotted against radial distance from the soma. Mean A$_{2B}$R fluorescent intensity was quantified in each ROI drawn around the βIII-Tubulin$^+$-DRGN soma in 3 random fields per coverslip using ROI 1-click tools. GFP-negative DRGNs were excluded from the analysis.

2.9 | Drugs

The A$_{2B}$R agonist 2-[[6-amino-3,5-dicyano-4-[4-(cyclopropylmethoxy)phenyl]-2-pyridinyl]thio]-acetamide (BAY60-6583; Tocris, UK, #4472), the A$_{2B}$R antagonist 8-(4-(4-(4-Chlorophenyl) piperazide-1-sulfonyl) phenyl)-1-propylxanthine (PSB-603; Merck, Germany, #3198), the A$_{2B}$R inverse agonist N-(4-Acetylphenyl)-2-[4-(2,3,6,7-tetrahydro-2,6-dioxo-1,3-dipropyl-1H-purin-8-yl)phenoxy]acetamide (MRS1706; Tocris, UK, #1584) were used. All drugs were dissolved in dimethyl sulphoxide (DMSO; Merck, Germany, #472301). Stock solutions, of 1,000–10,000 times the desired final concentration, were stored at −20°C. Control experiments demonstrated that the maximal DMSO concentration used in the present work (0.1%) was inactive in modulating membrane currents in DRGNs (data not shown).

2.10 | Statistics

All data were expressed as mean ± SEM (standard error of the mean). Normality distribution of data was checked by Shapiro–Wilk test. Two-tailed Student's paired t-tests and one-way ANOVA followed by appropriate posthoc test was performed as indicated in the figure legend in order to determine statistical significance (set at $p < .05$). Data were analyzed using GraphPad Prism 8th edition (GraphPad Software, San Diego, CA, USA) software.

3 | RESULTS

3.1 | Adenosine A$_{2B}$ receptor activation inhibits OPC differentiation and promotes myelination in dorsal root ganglion neuron/OPC cocultures

To determine the role of A$_{2B}$Rs during myelination in vitro, rat OPCs were cocultured with rat DRGNs ($n = 26$ from 13 OPC/DRGN cocultures) in the presence of the pro-differentiating T3 hormone (50 nM) to improve myelination (Calza et al., 2002). In the first series of experiments, we evaluated the time-dependence of myelination processes during cell growth by measuring different parameters in OPC/DRGN cocultures stained by myelin- and axon-targeting specific antibodies (MBP and βIII-tubulin, respectively). We also evaluated, at different times in culture, that is at 7-; 10-; 14-; and 21-days cocultures (t_7; t_{10}; t_{14}, and t_{21}, respectively) modifications in OL morphology, as indicated
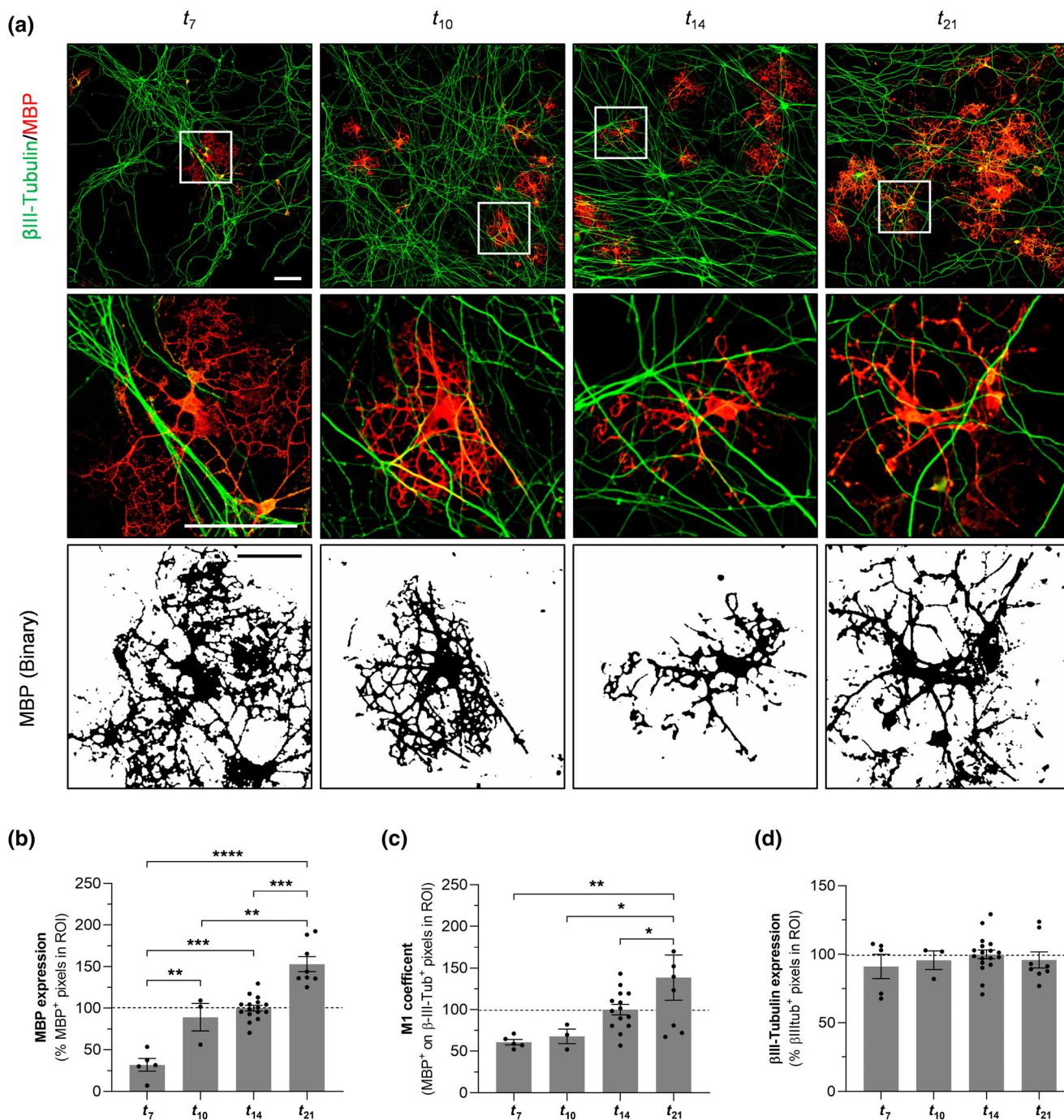
FIGURE 1   Time course of oligodendrocyte precursor cell (OPC) maturation in a dorsal root ganglion neuron (DRGN) and OPCs coculture model. (a) Upper panels: Representative images of OPC/DRGN coculture stained for myelin basic protein (MBP, red) and βIII-tubulin (green) at different time points (t_7, t_{10}, t_{14}, and t_{21}). Magnification: ×20. Scale bar = 50 μm. Middle panels: Magnification of the region of interest (ROI) indicated in the upper panels, to visualize overlapping between MBP and βIII-tubulin. Lower panels: MBP$^+$ images are converted into binary images to better clarify the oligodendrocyte morphology of the same ROI mentioned above. Scale bar = 25 μm. (b–d) Quantification of MBP (b) and βIII-tubulin (d) expression at different time points (t_7, t_{10}, t_{14}, and t_{21}). MBP is reported as percentage change to t_{14}. Values are expressed as mean ± SEM in different experimental conditions. (c) Mander's coefficient (M1 coefficient) quantified as the overlap of MBP$^+$ pixels on βIII-tubulin$^+$ pixels, is reported as percentage change to t_{14}. *$p < .05$; **$p < .01$; ***$p < .001$; ****$p < .0001$; Nested One-way ANOVA; Dunnet's posttest versus t_{14}.

both in microphotography and in corresponding binary images of MBP signal (Figure 1a). A progressive increase in MBP expression (Figure 1b) and M1 coefficient (Figure 1c) were observed from t_7 to t_{21}. No significant changes in βIII-Tubulin expression were observed at any time point investigated (Figure 1d). Based on these data, we investigated the effects of adenosinergic compounds in OPC/DRGN
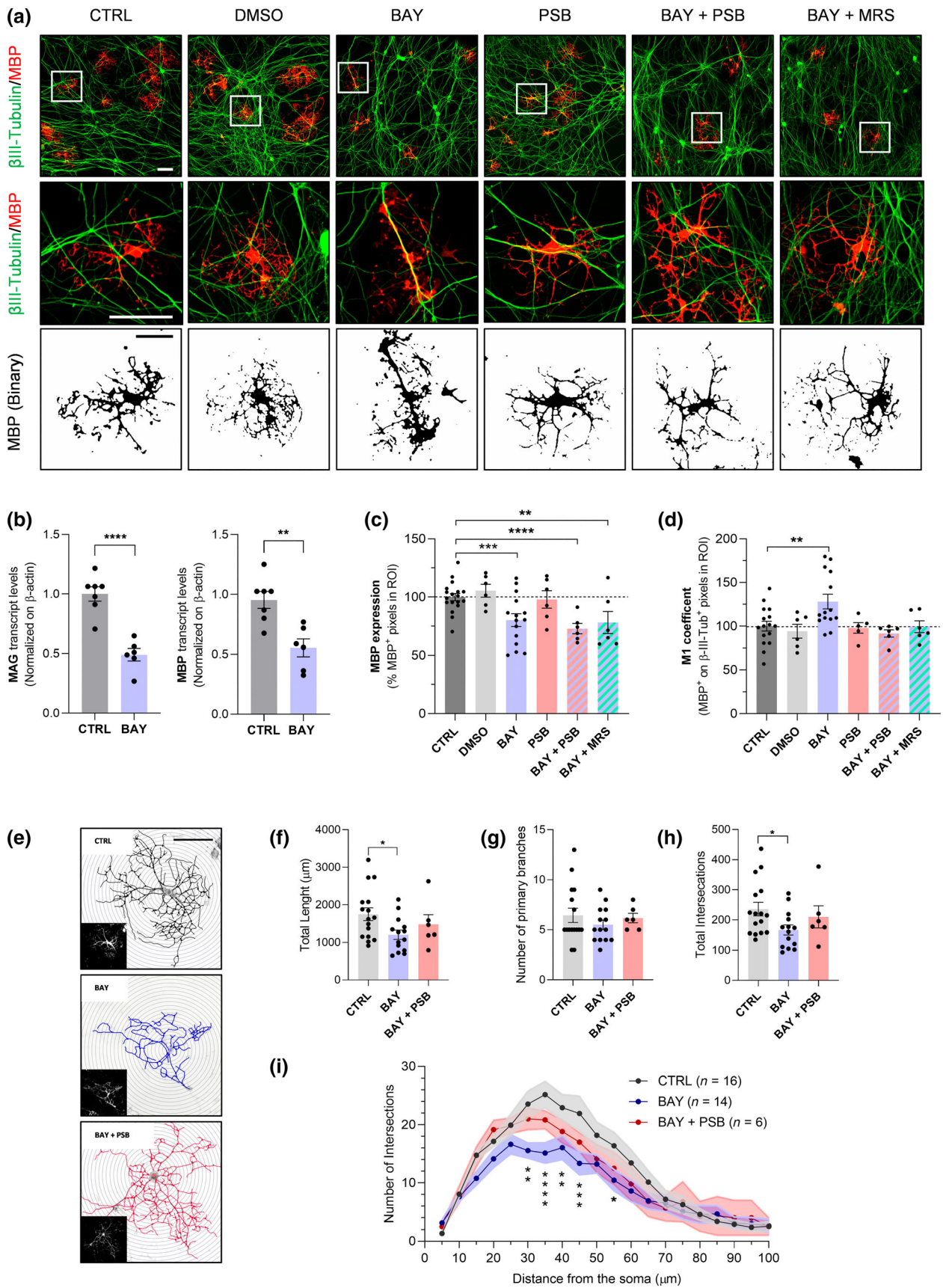
FIGURE 2 Legend on next page.

cocultures at t_{14}, as this is the time point at which oligodendrocyte morphology modifications, induced by pro- and anti-differentiating ligands, are more detectable.

As shown in Figure 2, the $A_{2B}R$ agonist BAY60-6583 (1 μM), added for 2 weeks in the culture medium, reduced MAG and MBP gene expression, as well MBP$^+$ cells, in OPC/DRGN cocultures (Figure 2b,c). This result demonstrates that the selective stimulation of this receptor subtype reduces OPC maturation, in accordance with our previous data obtained by using purified OPC cultures (Coppi, Cherchi, et al., 2020). However, this effect was not prevented by $A_{2B}R$ antagonists, MRS1706 (5 μM) and PSB-603 (10 nM; Figure 2a,c). Despite the decrease in MBP expression, we surprisingly observed a significant increase in M1 coefficient when cocultures were grown in the presence of BAY60-6583 (Figure 2a,c), indicating a higher degree of MBP signal aligned with βIII-Tubulin-positive neuronal processes, that is increased axonal myelination. Differently from what observed for total MBP expression, both the $A_{2B}R$ antagonists tested, MRS1706 (5 μM) and PSB-603 (10 nM), were able to prevent the increase in axonal myelination induced by BAY60-6583 (Figure 2c). In addition, OL morphology appears more compacted when cells were grown in the presence of BAY60-6583, in comparison to control conditions, as shown in binary images (Figure 2a). The morphological complexity of oligodendrocyte processes was quantified by Sholl analysis (Figure 2e–i). This analysis revealed significant differences in process complexity between control and BAY-treated cells. In particular, BAY60-6583 reduces total length of the ramification (Figure 2f) as well as the total number of intersections with Sholl rings (Figure 2h), without affecting the number of primary branches (Figure 2g). None of the tested compounds modified βIII-Tubulin expression (Figure S1).

These results indicate that $A_{2B}R$ activation could promote a more efficient axonal enwrapping by myelin sheaths, while reducing total MBP levels. This discrepancy could suggest a differential role of $A_{2B}Rs$ on myelin production depending on the site of expression of the receptor in the coculture.

## 3.2 | Adenosine $A_{2B}Rs$ are expressed on DRGNs where they enhance cell excitability

As first demonstrated by Li et al. (2022) in DRGNs innervating the acupoint Zusanli (ST36), we confirmed and expanded data demonstrating the expression of $A_{2B}Rs$ on DRGNs, as shown by immunofluorescence staining of DRGN monocultures (Figure 3).

In a second set of experiments, we investigated eventual effects induced by selective $A_{2B}R$ activation on the excitability of DRGNs by performing current-clamp recordings. To assess intrinsic excitability of DRGNs, we evoked AP discharge by current pulses of increasing amplitude (from −10 to +40 pA, 1200 ms). We found that, after 5-min of 1 μM BAY60-6583 application, the number of APs evoked by depolarizing inputs at +10 pA and +20 pA was significantly increased, as shown by the event frequency/current curve (Figure 4a,b). We then applied a single depolarizing step (+10 pA) every 15 s and we observed a significant effect of BAY60-6583 at 5-min application and this increase was reversible after washout (Figure 4c). In addition, we tested different concentrations of $A_{2B}R$ agonist (0.1–10 μM) and we found an increase in AP firing from 0.3 μM concentration (Figure 4d). As shown in Figure 4e,f, BAY60-6583 depolarized RMP in a concentration-dependent manner (0.1–10 μM) in isolated DRGNs, ($EC_{50} = 0.4$ μM; confidence limits: 0.15–0.97 μM), similar to our previous observations in OPC monocultures ($EC_{50} = 0.6$ μM; Coppi, Cherchi, et al., 2020).

In order to deepen the effect of BAY60-6583 on single AP waveform, we quantified the peak amplitude, half width, maximal rise slope and maximal decay slope before and after BAY60-6583 application (Figure 5a,b). We did not find significant changes in any of the AP parameter measured (Table 1). In addition, the increase in AP firing evoked by 1 μM BAY60-6583 was associated with a decrease in rheobase (from 5.63 ± 1.12 to 3.51 ± 0.65 pA) and in RMP (from −61.66 ± 1.84 to −57.72 ± 1.91 mV), thus confirming enhanced excitability (Figure 5c–e and Table 1). We observed a significant increase in input resistance (from 506.7 ± 102.0 to 583.3

FIGURE 2 Pharmacological activation of adenosine A_{2B} receptor reduces myelin basic protein expression but increases myelination coefficient in OPC/DRGN cocultures. (a) Representative images of OPC/DRGN cultures stained for myelin basic protein (MBP, red) and βIII-tubulin (green) in different experimental conditions: Control (CTRL); vehicle (DMSO 1:1000), 1 μM BAY60-6583 (BAY, a selective $A_{2B}R$ agonist), 10 nM PSB-603 (PSB, a selective $A_{2B}R$ antagonist), BAY + PSB and BAY + 5 μM MRS1706 (MRS, a selective $A_{2B}R$ antagonist). Magnification: ×20. Scale bar = 50 μm. Middle panels: Magnification of the region of interest (ROI) indicated in the upper panels. Lower panels: MBP$^+$ images are converted into binary images to better clarify the oligodendrocyte morphology of the ROI indicated in upper panels. Scale bar = 25 μm. (b) Effect of BAY on the gene expression of myelin associated glycoprotein (MAG; left panel) and MBP (right panel) in OPC/DRGN cocultures at t_{14}. Data were normalized to β-actin and reported as mean ± SEM of 5 independent experiments performed in duplicate. **$p < .01$; ****$p < .0001$; Unpaired Student t-test. (c) Quantification of MBP expression in different experimental conditions at t_{14}. MBP expression is reported as percentage change to CTRL at t_{14}. (d) Mander's coefficient (M1 coefficient), quantified as the overlap of MBP$^+$ pixels on βIII-tubulin$^+$ pixels, is reported as percentage change to CTRL at t_{14} in the same experimental conditions. **$p < .01$; ***$p < .001$; ****$p < .0001$; Nested One-way ANOVA; Dunnet's posttest versus CTRL group. (e) Sholl dendritic analysis of reconstructed oligodendrocytes in different experimental conditions. Scale bar: 50 μm. (f–h) Pooled data of different parameters measured by Sholl dendritic analysis of reconstructed oligodendrocytes in control (CTRL, gray columns, $n = 16$ from 8 independent experiments), BAY (blue columns, $n = 14$ from 7 independent experiments) and BAY coapplied with PSB (BAY + PSB, red columns, $n = 6$ from 3 independent experiments). *$p < .05$; One-way ANOVA; Dunnet's posttest versus CTRL group. (i) Plots of number of intersections as a function of Sholl distance from the oligodendrocyte soma in different experimental conditions: CTRL, BAY, and BAY + PSB. Data are expressed as mean ± SEM. **$p < .01$; ***$p < .001$; ****$p < .0001$; Two-way ANOVA; Dunnet's posttest versus CTRL group. Data are expressed as mean ± SEM.
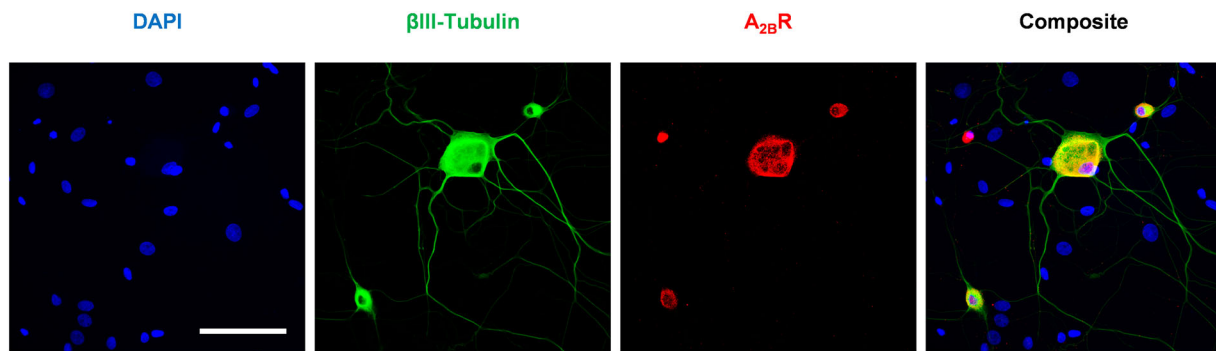
FIGURE 3 DRGNs express adenosine A_{2B} receptors. Confocal images of immunofluorescence staining for $A_{2B}R$ (red) and βIII-tubulin (green) in primary purified neuronal DRGN cultures. Cell nuclei are marked with DAPI (blue). Objective: ×63. Scale bar: 75 μm.

± 112.6 MΩ), that could indicate a channel closure (Figure 5f and Table 1). All these effects were prevented by the selective $A_{2B}R$ antagonist, PSB-603 (10 nM; Figure 5).

Altogether, these data demonstrate that $A_{2B}Rs$ are expressed on DRGNs where their activation increases neuronal firing. Hence, as neuronal firing is known to promote the release of chemoattractant/promyelinating factors for OPCs and/or OLs (Arellano et al., 2016; Barres & Raff, 1993, 1999; Duncan et al., 2021; Saab et al., 2016; Simons & Nave, 2015) this could be a mechanism by which BAY60-6583 increases myelination in DRGN/OPC cocultures, as observed in the present work.

To strengthen our hypothesis, we silenced $A_{2B}Rs$ by infecting DRGNs with AAV2/5 expressing a shRNA (short hairpin RNA) to target *Adora2B* and GFP as infection reporter (Mason et al., 2010) before adding OPCs. First, we confirmed that both the infection and the $A_{2B}R$ silencing have occurred by receptor expression analysis with immunofluorescence (reduction of 31.33 ± 5.21%; Figure 6a,b) and its transcript levels with RT-qPCR (reduction of 52.85 ± 15.72%; Figure 6c). Afterward, we added OPCs to DRGNs infected with AAV2/5 expressing shRNA against $A_{2B}R$ (sh$A_{2B}R$-DRGNs) and maintained the cocultures for 14 days in the absence or presence of BAY60-6583 (Figure 6d). In these conditions, the $A_{2B}R$ agonist reduced MBP levels, as expected upon the activation of this receptor expressed on OPCs alone (Figure 6e). MBP levels notwithstanding were increased in OPC/sh$A_{2B}R$-DRGN cocultures, but we are not yet in the position to explain this effect that surely needs to be deepened. However, given the notoriously low affinity of this receptor for the endogenous ligand adenosine, we exclude the hypothesis that $A_{2B}R$ could be activated by adenosine released in the DRGN/OPC cocultures under control conditions, since we did not observe any modification in MBP levels when the $A_{2B}R$ antagonist PSB-603 was applied alone (Figure 2). For the same reason, the constitutive activation of $A_{2B}R$ is also improbable. We cannot exclude the hypothesis that $A_{2B}Rs$, expressed on DRGNs, may interact with other G-proteins coupled receptors and/or alternative pathways that also modulate OPC differentiation. Hence, the lack of $A_{2B}Rs$ on DRGNs may change the overall balance of neuron-to-glial interaction and unmasks a pro-differentiating effect on OPCs. Moreover, in the OPC/sh$A_{2B}R$-DRGN cocultures, BAY60-6583 did not modify M1 coefficient (Figure 6e),

strengthening our hypothesis that the myelination increase was due to $A_{2B}R$ activation on DRGNs.

4 | DISCUSSION

In this study, we showed that $A_{2B}R$ activation decreases OPC differentiation but, on the other hand, increases myelination of DRGN axons cocultured with OPCs, probably by increasing neuronal activity.

Adenosine orchestrates several phases of oligodendrogliogenesis through the activation of its metabotropic receptors (A_1R, $A_{2A}R$, $A_{2B}R$, and A_3R) with different outcomes depending on the receptor subtype involved (Cherchi, Pugliese, & Coppi, 2021; Fields & Burnstock, 2006; Stevens et al., 2002). The $A_{2B}R$ is the most enigmatic P1 adenosine receptor, since its pharmacological and physiological characterization has long been precluded by the lack of suitable ligands (Coppi, Dettori, et al., 2020; Popoli & Pepponi, 2012). Little is known about the role of $A_{2B}Rs$ in oligodendrogliogenesis. Recently, we demonstrated that $A_{2B}Rs$ are expressed at each stage of oligodendrogliogenesis and the $A_{2B}R$ agonist, BAY60-6583, reversibly inhibits tetraethylammonium-(TEA-) sensitive, sustained I_K, and 4-aminopyridine- (4-AP) sensitive, transient I_A, conductances (Coppi, Cherchi, et al., 2020). It is known that these currents are necessary to OPC differentiation, and their modulation could represent an important target in demyelinating pathologies (Cherchi, Bulli, et al., 2021; Chittajallu et al., 2002, 2004; Gallo et al., 1996; Zhang et al., 2021). Indeed, BAY60-6583 also inhibited the differentiation of primary OPC cultures, as demonstrated by the reduced expression of MBP and MAG (Coppi, Cherchi, et al., 2020) after 7 days of OPCs culture growth in the presence of the compound. We have to consider that OPC monocultures recapitulate several features of OL differentiation, including the production of myelin components as MBP and MAG. However, they do not represent a myelination model due to the absence of neuronal axons (Marangon et al., 2021). For these reasons, we first wanted to deepen knowledge of the role of $A_{2B}Rs$ during myelination in DRGN/OPC cocultures, which represent a more sophisticated system than OPC monocultures.
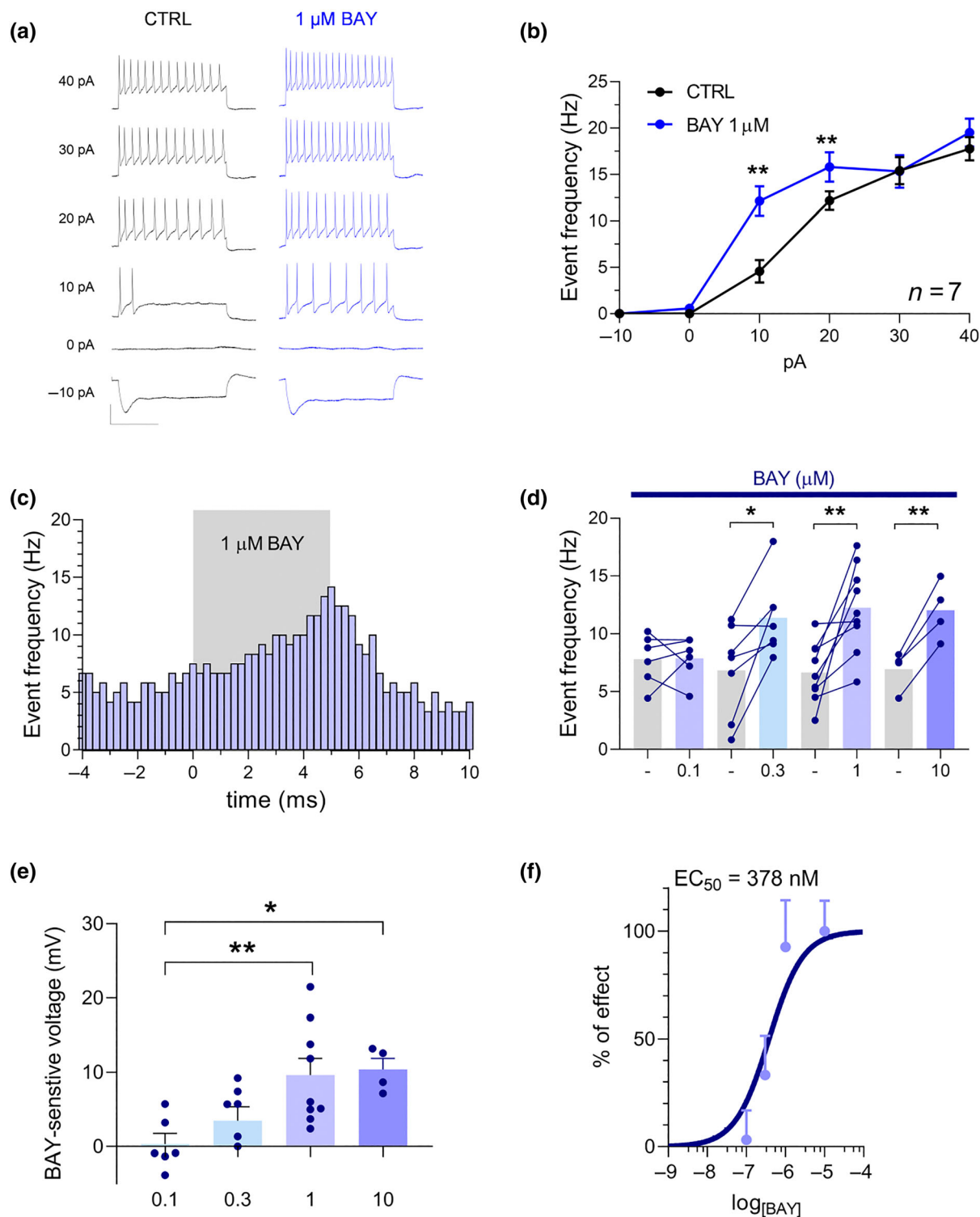
FIGURE 4 Stimulation of adenosine A_{2B} receptors increases action potential firing in primary neuronal DRGN cultures. (a) Original voltage traces evoked by a current-step protocol (from −10 to +40 pA, 1200 ms) in a representative DRGN before (black traces, left panels) or 5-min after the application of 1 μM BAY60-6583 (BAY: blue traces, right panels). (b) Averaged number of action potentials (APs)-to-current injected relationship recorded in the absence (CTRL: black circles) or in the presence (BAY: blue circles) of 1 μM BAY60-6583 in 7 cells investigated. **$p < .01$; paired Student's t-test. (c) Time course of firing rate evoked in a typical DRGN by a 1200 ms depolarizing step current injection 10 pA (every 30 s) recorded before, during and after 5-min 1 μM BAY60-6583 application. (d) Pooled data of AP frequency (event frequency; Hz) measured before or after a 5-min BAY60-6583 (0.1–10 μM) application. *$p < .05$; **$p < .01$; paired Student's t-test. (e) Pooled data of resting membrane potential (RMP) difference in absence or presence of BAY60-6583 (BAY-sensitive RMP) at different concentrations (0.1–10 μM). *$p < .05$; **$p < .01$ versus 0.1 μM BAY60-6583, one-way ANOVA, Dunnet's posttest. (f) Concentration-response curve of BAY60-6583 effect on RMP (expressed as percentage of baseline) in cultured DRGNs ($EC_{50} = 0.38$ μM, confidence limits: 0.15–0.97 μM). Data are expressed as mean ± SEM.
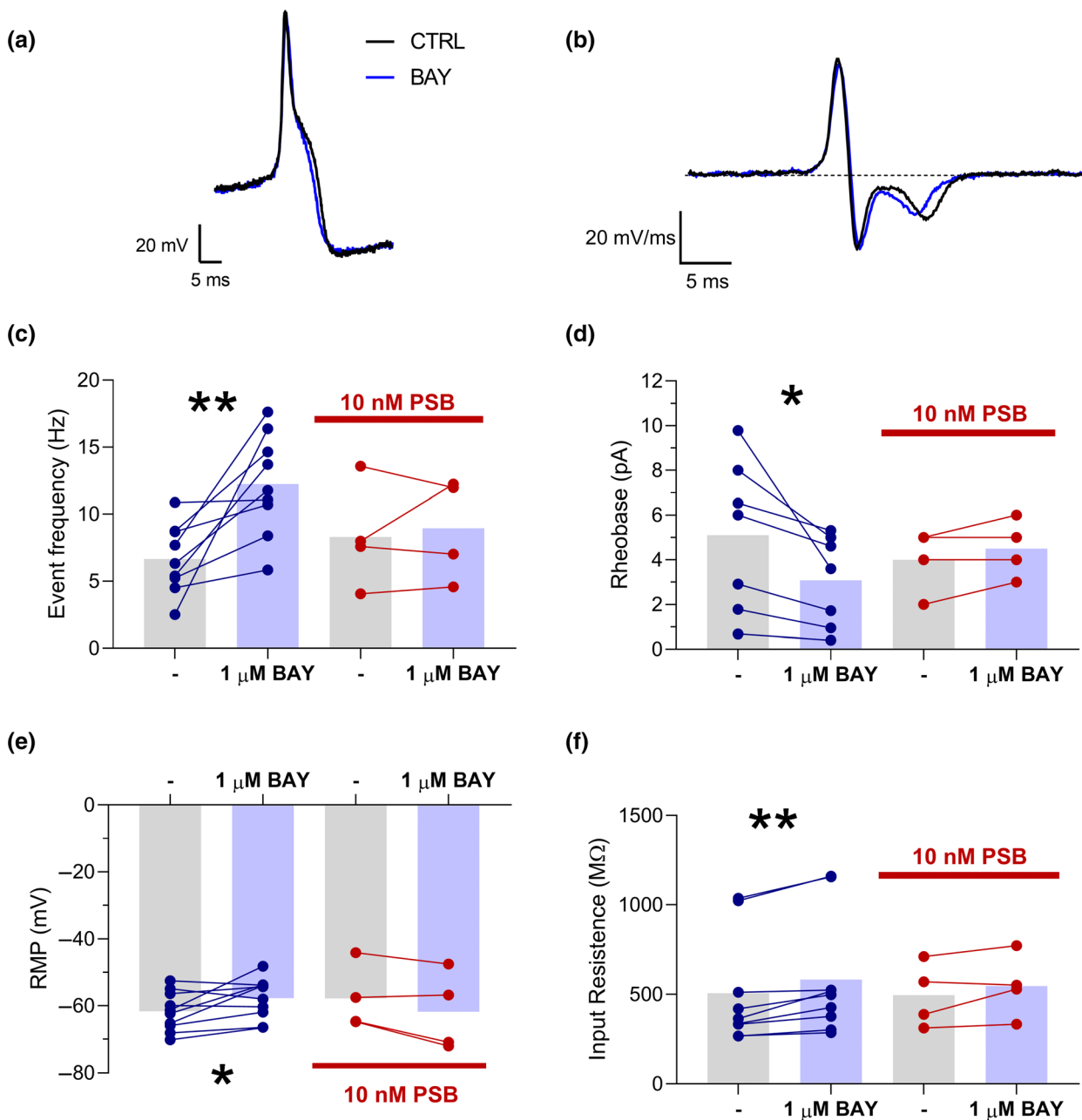
FIGURE 5 The selective adenosine A_{2B} receptor antagonist, PSB-603, prevents the effects induced by BAY60-6583 on different excitability parameters of isolated DRGNs. (a) Example traces of the third action potential (AP) waveform before (CTRL: black trace) and 5-min after 1 μM BAY60-6583 (BAY: blue trace) on an expanded time scale. (b) First derivate of voltage versus time (mV/ms) of AP traces represented in (a). (c–f) Pooled data of AP frequency (c), rheobase (d), resting membrane potential (RMP, e), and input resistance (f) measured before or after a 5-min 1 μM BAY application, alone or in the presence of the selective $A_{2B}R$ antagonist (0.01 μM PSB-603). *$p < .05$; **$p < .01$; Paired Student's t-test.

To this aim, we took advantage of a DRGN/OPC cocultures to quantify the level of MBP expression and myelination index (M1 coefficient). In this in vitro model, we observed, in the present research, a time-dependent increase both in MBP levels and M1 coefficient from t_7 to t_{21}. Then we chose t_{14} as our reference time point to evaluate the effects of different $A_{2B}R$ compounds, since at this time oligodendrocyte morphology modifications, induced by pro- and anti-differentiating ligands, are more detectable. First, we observed that the selective $A_{2B}R$ antagonist, PSB-603, did not modify MBP

levels nor M1 coefficients when added to the cocultures for 14 days, indicating that micromolar concentrations of adenosine, needed to activate the $A_{2B}R$ subtype, are not reached in our experimental model, that is in the absence of insults. In line with our previous data (Coppi, Cherchi, et al., 2020), we found that a chronic treatment (14 days) with the selective $A_{2B}R$ agonist BAY60-6583 reduces MBP expression, indicating a decreased OPC differentiation capacity. Nevertheless, even if minor in number, the OLs formed in the presence of the $A_{2B}R$ agonist were significantly more prone to myelinate axons in the

TABLE 1   Effects of BAY60-6583 on action potential properties in DRGNs.

	Bsl ($n = 9$)	1 μM BAY ($n = 9$)	P Student's paired t-test
Peak amplitude (mV)	89.0 ± 6.4	89.9 ± 5.6	0.847
Half width (ms)	6.8 ± 0.8	5.8 ± 0.9	0.174
Max rise slope (mV/ms)	88.3 ± 12.8	93.8 ± 11.8	0.533
Max decay slope (mV/ms)	−81.8 ± 10.0	−82.2 ± 11.0	0.999
Latency (ms)	210.4 ± 38.9	154.3 ± 20.6	*0.044
Rheobase (pA)	5.6 ± 1.1	3.5 ± 0.7	*0.019
RMP (mV)	−61.7 ± 1.8	−57.7 ± 1.9	*0.025
Input resistance (MΩ)	506.7 ± 102.0	583.3 ± 112.6	**0.001

Note: Each value is expressed as mean ± SEM before (bsl) and after 5-min BAY60-6583 (BAY, 1 μM) application. $*p < .05$; $**p < .01$; Paired Student's t-test.
Abbreviation: RMP, resting membrane potential.

coculture system compared with control conditions, as proved by the increase in M1 coefficient. Our results also showed that exposure to BAY60-6583 lead to a significant reduction in cellular arborization and morphological changes of oligodendrocytes (Barateiro et al., 2013; Simons & Nave, 2015).

It must be considered that oligodendrogliogenesis is a process finely tuned at different time points. Regarding myelination, OLs have to synthesise, sort and traffic a vast number of proteins in a short time (in the range of 12–18 h) (Barres, 2008; Bradl & Lassmann, 2010). For example, Fitzner and collaborators demonstrate that proteolipid protein (PLP), one of the major myelin-related proteins alongside MBP and MAG, is predominantly intracellular in OLs monocultures (Fitzner et al., 2006). However, when OLs are cocultured with neurons, PLP colocalized with MBP, indicating a higher density of myelin components exposed on the surface of OL membrane when neurons are present in the coculture (Bradl & Lassmann, 2010; Fitzner et al., 2006). Moreover, data in the literature demonstrate that OLs produce PLP in advance and store it intracellularly, until the onset of myelination stimulates its translocation to the membrane (Bradl & Lassmann, 2010; Simons & Trajkovic, 2006).

Interestingly, common $A_{2B}R$ antagonists, PSB-603 and MRS1706, are able to prevent the increased myelination index, but not the reduction in total MBP levels induced by BAY60-6583. We do not have any obvious explanation for the lack of effect of PSB-603 or MRS1706 on BAY60-6583-dependent reduction in total MBP levels. However, it appears from our data that the increase in axonal myelination index induced by BAY60-6583 is an event distinct from inhibition of OPC differentiation induced by the same

compound. Since $A_{2B}Rs$ are expressed either on OPCs or DRGNs, we can hypothesize that distinct effects of BAY60-6583 might emerge as a consequence of different cellular localization of this receptor subtype. In our experiments, the increase in myelination coefficient could be attributed to $A_{2B}Rs$ expressed on DRGNs, which are sensitive to PSB-603 antagonism, as confirmed by our patch-clamp recordings. On the contrary, the decrease in total MBP levels is likely due to the activation of $A_{2B}Rs$ expressed on OPCs, in line with our previous data on OPC monocultures (Coppi, Cherchi, et al., 2020), and this effect is not prevented by the tested antagonists. Hence, on these bases, we can hypothesize that neuronal $A_{2B}Rs$ are sensitive to common $A_{2B}R$ antagonists, in accordance with other data (Fusco et al., 2018, 2019), whereas oligodendroglial $A_{2B}Rs$ might present isoform/s with a different sensitivity to canonical antagonists. In confirm, Thimm and collaborators suggest that the lack of specific aminoacidic residues (i.e., Leu81) from $A_{2B}R$ could prevent the binding of some antagonists, especially for larger ligands such as PSB-603 (Thimm et al., 2013). Indeed, to our knowledge, no data are available in the literature about the block of BAY-mediated effects on oligodendroglial cells by PSB-603. Moreover, we cannot exclude that BAY60-6583 could have independent effects from the $A_{2B}R$ activation, as demonstrated in peripheral T cells (Tang et al., 2021).

To gain insight into the functional role of $A_{2B}R$ on neurons in our experimental model, we tested the unexplored effects of BAY60-6583 on primary DRGN monoculture excitability. We found that rat DRGNs expressed $A_{2B}Rs$, and its activation increases neuronal firing, decreases rheobase, depolarizes resting membrane potential and increases input resistance, indicating increased excitability and ionic channels closure. Other experiments are needed to identify the channel/s involved. All these effects were prevented in the presence of the selective $A_{2B}R$ antagonist, PSB-603. Since increased neuronal firing promotes the release of neurotransmitters (such as glutamate; Cherchi, Bulli, et al., 2021; Krasnow & Attwell, 2016; Zonouzi et al., 2011) and/or neuromodulators, the $A_{2B}R$ activation on DRGNs could promote OPC recruitment and myelination of actively firing axons in the OPC/DRGN cocultures.

For this purpose, we downregulated $A_{2B}Rs$ by infecting DRGNs with AAV2/5 expressing shRNA against $A_{2B}R$ (Mason et al., 2010) before adding OPCs, and maintaining the coculture for 14 days. In these experimental conditions, BAY60-6583 still induced a decrease in MBP expression but did not increase myelination of $shA_{2B}R$-DRGN axons. It therefore appears that the increase in myelination was due to the presence of $A_{2B}Rs$ on DRGNs, while the reduction in MBP levels was induced by the activation of this receptor subtype on OPCs. These findings consolidate our hypothesis about the differential role of $A_{2B}Rs$ depending on their cellular localization. Only few data in the literature reported the presence and/or functional effects of $A_{2B}Rs$ on neurons (Li et al., 2022; Wang et al., 2023). Wang and collaborators demonstrated that, in *Drosophila*, the activation of the only adenosine receptor subtype expressed (AdoR), a G_s-coupled receptor with high sequence similarity with $A_{2A}R$ and $A_{2B}R$, increases neuronal activity and axon
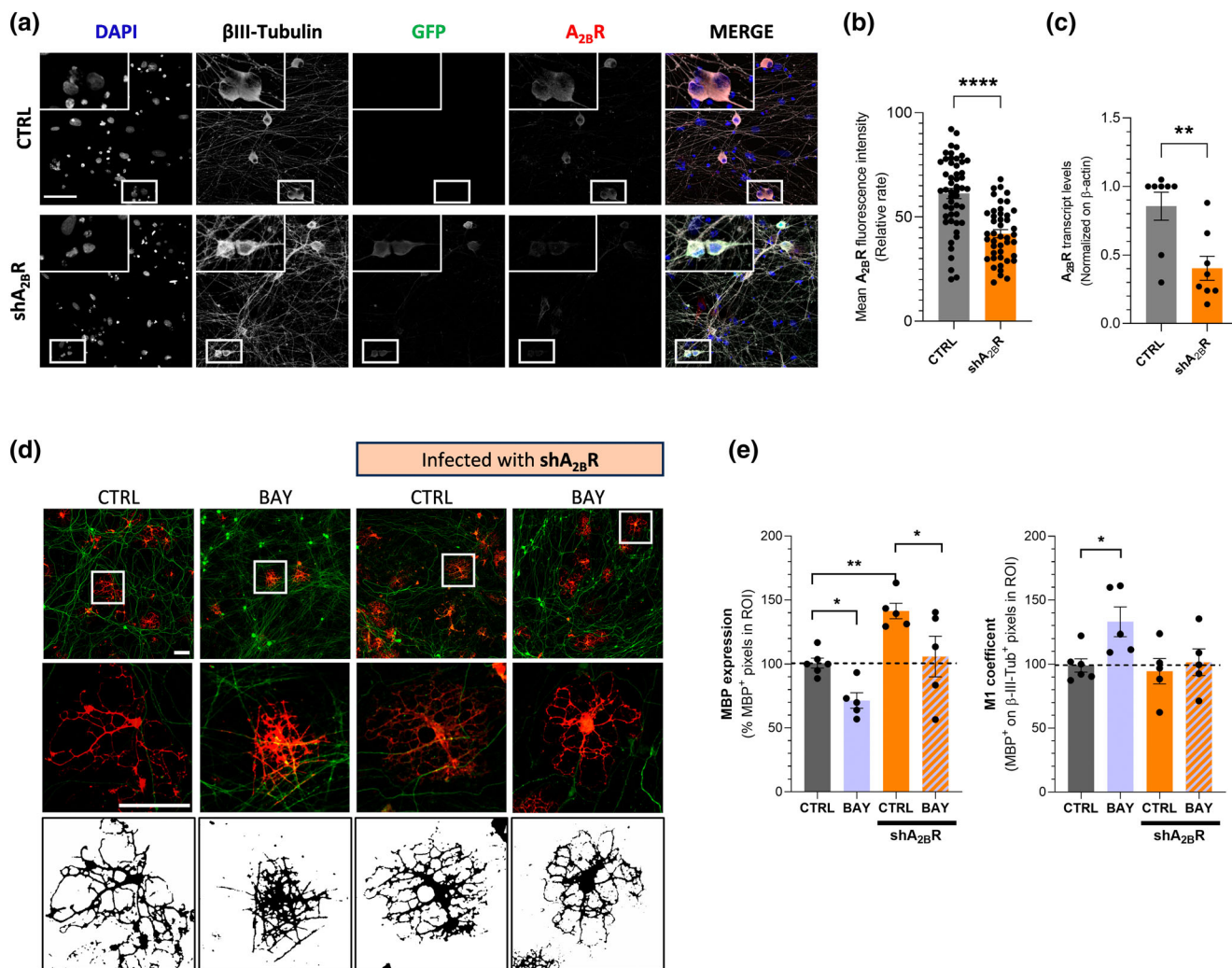
FIGURE 6 The downregulation of adenosine A_{2B} receptor in primary DRGNs prevents the increased myelination, but not the reduction in MBP expression, induced by BAY60-6583 in OPC/DRGN cocultures. (a) Representative $\times$63 fluorescent images staining for DAPI (blue), βIII-tubulin (gray), green fluorescence protein (GFP; green; used as reporter tag) and $A_{2B}R$ (red) in control (upper panels) or AAV-shA$_{2B}$ infected (shA$_{2B}$R; lower panels) DRGN monocultures. Scale bar: 75 μm. (b) Data for the mean fluorescent intensity of $A_{2B}R$ (red) was quantified as mean $\pm$ SEM of at least 5 neurons per image in 3 individuals replicates in control (CTRL; $n = 51$) or cultures infected with shA$_{2B}$R (shA$_{2B}$R; $n = 44$). ****$p < .0001$ unpaired Student t-test. (c) Quantification of the gene expression of $A_{2B}R$ normalized to β-actin. Data were reported as mean $\pm$ SEM of 5 independent experiments performed in duplicate. *$p < .05$ by unpaired Student t-test. (d) Upper panels: Representative images of OPC/DRGN coculture stained for myelin basic protein (MBP, red) and βIII-tubulin (green) where DRGNs were or were not transfected with AAV-shA$_{2B}$R from 3 independent experiments. Magnification: $\times$20. Scale bar = 50 μm. Middle panels: Magnification of the ROI indicated in the upper panels. Lower panels: MBP$^+$ images are converted into binary images to better clarify the oligodendrocyte morphology of the ROI indicated in upper panels. Scale bar = 25 μm. (e) Quantification of MBP expression (left panel) and M1 coefficient (right panel) in different experimental condition. *$p < .05$; **$p < .01$; Nested One-way ANOVA; Dunnet's posttest.

regeneration (Wang et al., 2023). In the same article, the activation of $A_{2B}R$ also promotes axon regeneration and survival in retinal ganglion cells of adult mice. Furthermore, Li and collaborators found the immune signal for $A_{2B}Rs$ in rat ST36 DRGNs, which represents neurons innervating acupoints in L4 and L6 DRGNs, where its activation by BAY60-6583 inhibited outward delayed rectifier potassium currents in 53.57% of cells (Li et al., 2022). It is worth to note that the block of potassium channels is coherent with the increased neuronal excitability, depolarized RMP and increased input resistance of DRGNs induced by BAY60-6583 in the present work.

In conclusion, we demonstrate here that chronic (t_{14}) BAY60-6583 treatment decreases MBP levels and increases axon myelination in OPC/DRGN cocultures. This last effect was prevented by the downregulation of $A_{2B}Rs$ on DRGNs. Furthermore, acute (5-min) BAY60-6583 application increases neuronal excitability in primary DRGN monocultures. Above data could be accounted for the fact that: (1) activation of $A_{2B}Rs$ expressed on OPCs prevents their differentiation, indicated by a decrease in MBP expression, and (2) activation of $A_{2B}R$ on DRGNs increases their excitability, promoting OPC recruitment, differentiation, and myelination possibly by releasing pro-myelinating factors.

AUTHOR CONTRIBUTIONS

F.C., E.C., and A.M.P. conceptualized the project. F.C. designed experiments and analyzed the data with support of M.V., G.M., and L.F. F.C., M.V., G.M., M.C., and D.B. performed the experiments. C.S. provided technical assistance. F.C., M.V., G.M., E.C., and A.M.P. wrote the paper. All authors reviewed, corrected, and edited the manuscript. A.M.P., E.C., F.R., and F.D.L. supervised the work.

DATA AVAILABILITY STATEMENT

The data that support the findings of this study are available from the corresponding author upon reasonable request.

ORCID

Federica Cherchi https://orcid.org/0000-0001-6742-456X
Martina Venturini https://orcid.org/0000-0002-8198-4683
Giada Magni https://orcid.org/0000-0003-2736-9150
Lucia Frulloni https://orcid.org/0009-0007-0991-3390
Martina Chieca https://orcid.org/0000-0002-0247-9938
Daniela Buonvicino https://orcid.org/0000-0003-0435-8475
Clara Santalmasi https://orcid.org/0009-0000-7521-3121
Francesca Rossi https://orcid.org/0000-0002-1199-8019
Francesco De Logu https://orcid.org/0000-0001-8360-6929
Elisabetta Coppi https://orcid.org/0000-0003-4434-5919
Anna Maria Pugliese https://orcid.org/0000-0001-7554-5740

REFERENCES

Antonioli, L., Blandizzi, C., Pacher, P., & Haskó, G. (2013). Immunity, inflammation and cancer: A leading role for adenosine. *Nature Reviews Cancer, 13*, 842–857. www.nature.com/reviews/cancer

Arellano, R. O., Sánchez-Gómez, M. V., Alberdi, E., Canedo-Antelo, M., Chara, J. C., Palomino, A., Pérez-Samartín, A., & Matute, C. (2016). Axon-to-glia interaction regulates gabaa receptor expression in oligodendrocytes. *Molecular Pharmacology, 89*, 63–74. https://pubmed.ncbi.nlm.nih.gov/26538574/

Attali, B., Wang, N., Kolot, A., Sobko, A., Cherepanov, V., & Soliven, B. (1997). Characterization of delayed rectifier Kv channels in oligodendrocytes and progenitor cells. *Journal of Neuroscience, 17*, 8234–8245.

Barateiro, A., Miron, V. E., Santos, S. D., Relvas, J. B., Fernandes, A., Ffrench-Constant, C., & Brites, D. (2013). Unconjugated bilirubin restricts oligodendrocyte differentiation and axonal myelination. *Molecular Neurobiology, 47*, 632–644. https://pubmed.ncbi.nlm.nih.gov/23086523/

Barres, B. A. (2008). The mystery and magic of glia: A perspective on their roles in health and disease. *Neuron, 60*, 430–440. https://pubmed.ncbi.nlm.nih.gov/18995817/

Barres, B. A., & Raff, M. C. (1993). Proliferation of oligodendrocyte precursor cells depends on electrical activity in axons. *Nature, 361*, 258–260. https://www.nature.com/articles/361258a0

Barres, B. A., & Raff, M. C. (1999). Axonal control of oligodendrocyte development. *Journal of Cell Biology, 147*, 1123–1128. http://www.jcb.org

Bergles, D. E., Roberts, J. D. B., Somogyl, P., & Jahr, C. E. (2000). Glutamatergic synapses on oligodendrocyte precursor cells in the hippocampus. *Nature, 405*, 187–191. https://pubmed.ncbi.nlm.nih.gov/10821275/

Bolte, S., & Cordelières, F. P. (2006). A guided tour into subcellular colocalization analysis in light microscopy. *Journal of Microscopy, 224*, 213–232. https://pubmed.ncbi.nlm.nih.gov/17210054/

Bradl, M., & Lassmann, H. (2010). Oligodendrocytes: Biology and pathology. *Acta Neuropathologica, 119*, 37–53. https://pubmed.ncbi.nlm.nih.gov/19847447/

Buonvicino, D., Urru, M., Muzzi, M., Ranieri, G., Luceri, C., Oteri, C., Lapucci, A., & Chiarugi, A. (2018). Trigeminal ganglion transcriptome analysis in 2 rat models of medication-overuse headache reveals coherent and widespread induction of pronociceptive gene expression patterns. *Pain, 159*, 1980–1988. https://pubmed.ncbi.nlm.nih.gov/29794878/

Calza, L., Fernandez, M., Giuliani, A., Aloe, L., & Giardino, L. (2002). Thyroid hormone activates oligodendrocyte precursors and increases a myelin-forming protein and NGF content in the spinal cord during experimental allergic encephalomyelitis. *Proceedings of the National Academy of Sciences of the United States of America, 99*, 3258–3263. https://pubmed.ncbi.nlm.nih.gov/11867745/

Chan, J. R., Watkins, T. A., Cosgaya, J. M., Zhang, C., Chen, L., Reichardt, L. F., Shooter, E. M., & Barres, B. A. (2004). NGF controls axonal receptivity to myelination by Schwann cells or oligodendrocytes. *Neuron, 43*, 183–191. https://pubmed.ncbi.nlm.nih.gov/15260955/

Cherchi, F., Bulli, I., Venturini, M., Pugliese, A. M., & Coppi, E. (2021). Ion channels as new attractive targets to improve re-myelination processes in the brain. *International Journal of Molecular Sciences, 22*, 7277 https://pubmed.ncbi.nlm.nih.gov/34298893/

Cherchi, F., Pugliese, A. M., & Coppi, E. (2021). Oligodendrocyte precursor cell maturation: Role of adenosine receptors. *Neural Regeneration Research, 16*, 1686 http://www.nrronline.org/text.asp?2021/16/9/1686/306058

Chittajallu, R., Aguirre, A., & Gallo, V. (2004). NG2-positive cells in the mouse white and grey matter display distinct physiological properties. *Journal of Physiology, 561*, 109–122. https://pubmed.ncbi.nlm.nih.gov/15358811/

Chittajallu, R., Chen, Y., Wang, H., Yuan, X., Ghiani, C. A., Heckman, T., McBain, C. J., & Gallo, V. (2002). Regulation of Kv1 subunit expression in oligodendrocyte progenitor cells and their role in G 1/S phase progression of the cell cycle. *Proceedings of the National Academy of Sciences of the United States of America, 99*, 2350–2355.

Christofi, F. L., Zhang, H., Yu, J. G., Guzman, J., Xue, J., Kim, M., Wang, Y. Z., & Cooke, H. J. (2001). Differential gene expression of adenosine A1, A2a, A2b, and A3 receptors in the human enteric nervous system. *The Journal of Comparative Neurology, 439*, 46–64. https://pubmed.ncbi.nlm.nih.gov/11579381/

Cohen, C. C. H., Popovic, M. A., Klooster, J., Weil, M. T., Möbius, W., Nave, K. A., & Kole, M. H. P. (2020). Saltatory conduction along myelinated axons involves a periaxonal nanocircuit. *Cell, 180*, 311–322.e15.

Coppi, E., Cherchi, F., Fusco, I., Dettori, I., Gaviano, L., Magni, G., Catarzi, D., Colotta, V., Varano, F., Rossi, F., Bernacchioni, C.,

Donati, C., Bruni, P., Pedata, F., Cencetti, F., & Pugliese, A. M. (2020). Adenosine A2B receptors inhibit K+ currents and cell differentiation in cultured oligodendrocyte precursor cells and modulate sphingosine-1-phosphate signaling pathway. *Biochemical Pharmacology*, *177*, 113956 https://pubmed.ncbi.nlm.nih.gov/32251679/

Coppi, E., Cherchi, F., Fusco, I., Failli, P., Vona, A., Dettori, I., Gaviano, L., Lucarini, E., Jacobson, K. A., Tosh, D. K., Salvemini, D., Ghelardini, C., Pedata, F., Di Cesare, M. L., & Pugliese, A. M. (2019). Adenosine A3 receptor activation inhibits pronociceptive N-type Ca2+ currents and cell excitability in dorsal root ganglion neurons. *Pain*, *160*, 1103–1118. https://pubmed.ncbi.nlm.nih.gov/31008816/

Coppi, E., Dettori, I., Cherchi, F., Bulli, I., Venturini, M., Lana, D., Giovannini, M. G., Pedata, F., & Pugliese, A. M. (2020). A2b adenosine receptors: When outsiders may become an attractive target to treat brain ischemia or demyelination. *International Journal of Molecular Sciences*, *21*, 9697 https://www.mdpi.com/1422-0067/21/24/9697

Coppi, E., Maraula, G., Fumagalli, M., Failli, P., Cellai, L., Bonfanti, E., Mazzoni, L., Coppini, R., Abbracchio, M. P., Pedata, F., & Pugliese, A. M. (2013). UDP-glucose enhances outward K$^+$ currents necessary for cell differentiation and stimulates cell migration by activating the GPR17 receptor in oligodendrocyte precursors. *Glia*, *61*, 1155–1171. https://doi.org/10.1002/glia.22506

Corset, V., Nguyen-Ba-Charvet, K. T., Forcet, C., Moyse, E., Chédotal, A., & Mehlen, P. (2000). Netrin-1-mediated axon outgrowth and cAMP production requires interaction with adenosine A2b receptor. *Nature*, *407*, 747–750. https://www.nature.com/articles/35037600

De Biase, L. M., Kang, S. H., Baxi, E. G., Fukaya, M., Pucak, M. L., Mishina, M., Calabresi, P. A., & Bergles, D. E. (2011). NMDA receptor signaling in oligodendrocyte progenitors is not required for oligodendrogenesis and myelination. *Journal of Neuroscience*, *31*, 12650–12662. https://pubmed.ncbi.nlm.nih.gov/21880926/

De Biase, L. M., Nishiyama, A., & Bergles, D. E. (2010). Excitability and synaptic communication within the oligodendrocyte lineage. *Journal of Neuroscience*, *30*, 3600–3611. https://www.jneurosci.org/content/30/10/3600

Duncan, G. J., Simkins, T. J., & Emery, B. (2021). Neuron-oligodendrocyte interactions in the structure and integrity of axons. *Frontiers in Cell and Developmental Biology*, *9*, 460. https://doi.org/10.3389/fcell.2021.653101/full

Fannon, J., Tarmier, W., & Fulton, D. (2015). Neuronal activity and AMPA-type glutamate receptor activation regulates the morphological development of oligodendrocyte precursor cells. *Glia*, *63*, 1021–1035. https://pubmed.ncbi.nlm.nih.gov/25739948/

Fields, R. D. (2004). Volume transmission in activity-dependent regulation of myelinating glia. *Neurochemistry International*, *45*, 503–509.

Fields, R. D., & Burnstock, G. (2006). Purinergic signalling in neuron-glia interactions. *Nature Reviews. Neuroscience*, *7*, 423–436.

Fitzner, D., Schneider, A., Kippert, A., Möbius, W., Willig, K. I., Hell, S. W., Bunt, G., Gaus, K., & Simons, M. (2006). Myelin basic protein-dependent plasma membrane reorganization in the formation of myelin. *The EMBO Journal*, *25*, 5037–5048. https://pubmed.ncbi.nlm.nih.gov/17036049/

Forbes, T. A., & Gallo, V. (2017). All wrapped up: Environmental effects on myelination. *Trends in Neurosciences*, *40*, 572–587. https://pubmed.ncbi.nlm.nih.gov/28844283/

Fredholm, B. B., IJzerman, A. P., Jacobson, K. A., Linden, J., & Muller, C. E. (2011). International union of basic and clinical pharmacology. LXXXI. Nomenclature and classification of adenosine receptors—An update. *Pharmacological Reviews*, *63*, 1–34. http://www.ncbi.nlm.nih.gov/pubmed/21303899

Fusco, I., Cherchi, F., Catarzi, D., Colotta, V., Varano, F., Pedata, F., Pugliese, A. M., & Coppi, E. (2019). Functional characterization of a novel adenosine A2B receptor agonist on short-term plasticity and synaptic inhibition during oxygen and glucose deprivation in the rat CA1 hippocampus. *Brain Research Bulletin*, *151*, 174–180.

Fusco, I., Ugolini, F., Lana, D., Coppi, E., Dettori, I., Gaviano, L., Nosi, D., Cherchi, F., Pedata, F., Giovannini, M. G., & Pugliese, A. M. (2018). The selective antagonism of adenosine A2B receptors reduces the synaptic failure and neuronal death induced by oxygen and glucose deprivation in rat CA1 hippocampus in vitro. *Frontiers in Pharmacology*, *9*, 399.

Gallo, V., Mangin, J.-M., Kukley, M., & Dietrich, D. (2008). Synapses on NG2-expressing progenitors in the brain: Multiple functions? *The Journal Of Physiology*, *586*, 3767–3781. https://doi.org/10.1113/jphysiol.2008.158436

Gallo, V., Zhou, J. M., McBain, C. J., Wright, P., Knutson, P. L., & Armstrong, R. C. (1996). Oligodendrocyte progenitor cell proliferation and lineage progression are regulated by glutamate receptor-mediated K+ channel block. *Journal of Neuroscience*, *16*, 2659–2670. https://pubmed.ncbi.nlm.nih.gov/8786442/

Gensel, J. C., Schonberg, D. L., Alexander, J. K., McTigue, D. M., & Popovich, P. G. (2010). Semi-automated Sholl analysis for quantifying changes in growth and differentiation of neurons and glia. *Journal of Neuroscience Methods*, *190*, 71–79.

Gerace, E., Ilari, A., Caffino, L., Buonvicino, D., Lana, D., Ugolini, F., Resta, F., Nosi, D., Grazia Giovannini, M., Ciccocioppo, R., Fumagalli, F., Pellegrini-Giampietro, D. E., Masi, A., & Mannaioni, G. (2021). Ethanol neurotoxicity is mediated by changes in expression, surface localization and functional properties of glutamate AMPA receptors. *Journal of Neurochemistry*, *157*, 2106–2118. https://doi.org/10.1111/jnc.15223

Gonçalves, F. Q., Pires, J., Pliassova, A., Beleza, R., Lemos, C., Marques, J. M., Rodrigues, R. J., Canas, P. M., Köfalvi, A., Cunha, R. A., & Rial, D. (2015). Adenosine A2b receptors control A1 receptor-mediated inhibition of synaptic transmission in the mouse hippocampus. *European Journal of Neuroscience*, *41*, 876–886. https://pubmed.ncbi.nlm.nih.gov/25704806/

Igado, O. O., Andrioli, A., Azeez, I. A., Girolamo, F., Errede, M., Aina, O. O., Glaser, J., Holzgrabe, U., Bentivoglio, M., & Olopade, J. O. (2020). The ameliorative effects of a phenolic derivative of Moringa oleifera leave against vanadium-induced neurotoxicity in mice. *IBRO Neuroscience Reports*, *9*, 164–182.

Krasnow, A. M., & Attwell, D. (2016). NMDA receptors: Power switches for oligodendrocytes. *Neuron*, *91*, 3–5. https://pubmed.ncbi.nlm.nih.gov/27387644/

Kuhn, S., Gritti, L., Crooks, D., & Dombrowski, Y. (2019). Oligodendrocytes in development, myelin generation and beyond. *Cells*, *8*, 1424 https://pubmed.ncbi.nlm.nih.gov/31726662/

Kukley, M., Nishiyama, A., & Dietrich, D. (2010). The fate of synaptic input to NG2 glial cells: Neurons specifically downregulate transmitter release onto differentiating oligodendroglial cells. *Journal of Neuroscience*, *30*, 8320–8331. https://www.jneurosci.org/content/30/24/8320

Landini, L., Marini, M., Monteiro, S., de Araujo, D., Romitelli, A., Montini, M., Albanese, V., Titiz, M., Innocenti, A., Bianchini, F., Geppetti, P., Nassini, R., & De Logu, F. (2023). Schwann cell insulin-like growth factor receptor type-1 mediates metastatic bone cancer pain in mice. *Brain, Behavior, and Immunity*, *110*, 348–364. https://pubmed.ncbi.nlm.nih.gov/36940752/

Latini, S., & Pedata, F. (2001). Adenosine in the central nervous system: Release mechanisms and extracellular concentrations. *Journal of Neurochemistry*, *79*, 463–484. https://doi.org/10.1046/j.1471-4159.2001.00607.x

Lee, X., Yang, Z., Shao, Z., Rosenberg, S. S., Levesque, M., Pepinsky, R. B., Qiu, M., Miller, R. H., Chan, J. R., & Mi, S. (2007). NGF regulates the expression of axonal LINGO-1 to inhibit oligodendrocyte differentiation and myelination. *Journal of Neuroscience*, *27*, 220–225. https://www.jneurosci.org/content/27/1/220

Li, C., Xiao, L., Liu, X., Yang, W., Shen, W., Hu, C., Yang, G., & He, C. (2013). A functional role of NMDA receptor in regulating the differentiation of oligodendrocyte precursor cells and remyelination. *Glia*, *61*, 732–749. https://pubmed.ncbi.nlm.nih.gov/23440860/

Li, W., Dai, D., Chen, A., Gao, X. F., & Xiong, L. (2022). Characteristics of zusanli dorsal root ganglion neurons in rats and their receptor mechanisms in response to adenosine. *The Journal of Pain*, *23*, 1564–1580. https://pubmed.ncbi.nlm.nih.gov/35472520/

Lundgaard, I., Luzhynskaya, A., Stockley, J. H., Wang, Z., Evans, K. A., Swire, M., Volbracht, K., Gautier, H. O. B., Franklin, R. J. M., Ffrench-Constant, C., Attwell, D., & Káradóttir, R. T. (2013). Neuregulin and BDNF induce a switch to NMDA receptor-dependent myelination by oligodendrocytes. *PLoS Biology*, *11*, e1001743. https://doi.org/10.1371/journal.pbio.1001743

Ma, Q., Wang, D., Li, Y., Yang, H., Li, Y., Wang, J., Li, J., Sun, J., & Liu, J. (2022). Activation of A2B adenosine receptor protects against demyelination in a mouse model of schizophrenia. *Experimental and Therapeutic Medicine*, *23*, 396.

Manalo, J. M., Liu, H., Ding, D., Hicks, J., Sun, H., Salvi, R., Kellems, R. E., Pereira, F. A., & Xia, Y. (2020). Adenosine A2B receptor: A pathogenic factor and a therapeutic target for sensorineural hearing loss. *FASEB Journal*, *34*, 15771–15787. https://pubmed.ncbi.nlm.nih.gov/33131093/

Marangon, D., Caporale, N., Boccazzi, M., Abbracchio, M. P., Testa, G., & Lecca, D. (2021). Novel in vitro experimental approaches to study myelination and remyelination in the central nervous system. *Frontiers in Cellular Neuroscience*, *15*, 748849.

Marinelli, C., Bertalot, T., Zusso, M., Skaper, S. D., & Giusti, P. (2016). Systematic review of pharmacological properties of the oligodendrocyte lineage. *Frontiers in Cellular Neuroscience*, *10*, 27 https://pubmed.ncbi.nlm.nih.gov/26903812/

Mason, M. R. J., Ehlert, E. M. E., Eggers, R., Pool, C. W., Hermening, S., Huseinovic, A., Timmermans, E., Blits, B., & Verhaagen, J. (2010). Comparison of AAV serotypes for gene delivery to dorsal root ganglion neurons. *Molecular Therapy*, *18*, 715–724.

Meyer, N., Richter, N., Fan, Z., Siemonsmeier, G., Pivneva, T., Jordan, P., Steinhäuser, C., Semtner, M., Nolte, C., & Kettenmann, H. (2018). Oligodendrocytes in the mouse corpus callosum maintain axonal function by delivery of glucose. *Cell Reports*, *22*, 2383–2394. https://pubmed.ncbi.nlm.nih.gov/29490274/

Pedata, F., Dettori, I., Coppi, E., Melani, A., Fusco, I., Corradetti, R., & Pugliese, A. M. (2016). Purinergic signalling in brain ischemia. *Neuropharmacology*, *104*, 105–130. https://pubmed.ncbi.nlm.nih.gov/26581499/

Philips, T., & Rothstein, J. D. (2017). Oligodendroglia: Metabolic supporters of neurons. *Journal of Clinical Investigation*, *127*, 3271–3280. https://pubmed.ncbi.nlm.nih.gov/28862639/

Popoli, P., & Pepponi, R. (2012). Potential therapeutic relevance of adenosine A2B and A2A receptors in the central nervous system. *CNS & Neurological Disorders—Drug Targets*, *11*, 664–674. https://pubmed.ncbi.nlm.nih.gov/22963436/

Saab, A. S., Tzvetavona, I. D., Trevisiol, A., Baltan, S., Dibaj, P., Kusch, K., Möbius, W., Goetze, B., Jahn, H. M., Huang, W., Steffens, H., Schomburg, E. D., Pérez-Samartín, A., Pérez-Cerdá, F., Bakhtiari, D., Matute, C., Löwel, S., Griesinger, C., Hirrlinger, J., ... Nave, K. A. (2016). Oligodendroglial NMDA receptors regulate glucose import and axonal energy metabolism. *Neuron*, *91*, 119–132.

Schneider, C. A., Rasband, W. S., & Eliceiri, K. W. (2012). NIH image to ImageJ: 25 years of image analysis. *Nature Methods*, *9*, 671–675. https://www.nature.com/articles/nmeth.2089

Simons, M., & Nave, K. A. (2015). Oligodendrocytes: Myelination and axonal support. *Cold Spring Harbor Perspectives in Biology* https://pubmed.ncbi.nlm.nih.gov/26101081/, *8*, a020479.

Simons, M., & Trajkovic, K. (2006). Neuron-glia communication in the control of oligodendrocyte function and myelin biogenesis. *Journal of Cell Science*, *119*, 4381–4389. https://pubmed.ncbi.nlm.nih.gov/17074832/

Stevens, B., Porta, S., Haak, L. L., Gallo, V., & Fields, R. D. (2002). Adenosine: A neuron-glial transmitter promoting myelination in the CNS in response to action potentials. *Neuron*, *36*, 855–868.

Suminaite, D., Lyons, D. A., & Livesey, M. R. (2019). Myelinated axon physiology and regulation of neural circuit function. *Glia*, *67*, 2050–2062.

Sun, W., Matthews, E. A., Nicolas, V., Schoch, S., & Dietrich, D. (2016). Ng2 glial cells integrate synaptic input in global and dendritic calcium signals. *eLife*, *5*, e16262.

Tang, J., Zou, Y., Li, L., Lu, F., Xu, H., Ren, P., Bai, F., Niedermann, G., & Zhu, X. (2021). BAY 60-6583 enhances the antitumor function of chimeric antigen receptor-modified T cells independent of the adenosine A2b receptor. *Frontiers in Pharmacology*, *12*, 619800 www.frontiersin.org

Tepavčević, V., & Lubetzki, C. (2022). Oligodendrocyte progenitor cell recruitment and remyelination in multiple sclerosis: The more, the merrier? *Brain*, *145*, 4178–4192. https://doi.org/10.1093/brain/awac307

Thimm, D., Schiedel, A. C., Sherbiny, F. F., Hinz, S., Hochheiser, K., Bertarelli, D. C. G., Maaß, A., & Müller, C. E. (2013). Ligand-specific binding and activation of the human adenosine A(2B) receptor. *Biochemistry*, *52*, 726–740. https://pubmed.ncbi.nlm.nih.gov/23286920/

Vaes, J. E. G., Brandt, M. J. V., Wanders, N., Benders, M. J. N. L., de Theije, C. G. M., Gressens, P., & Nijboer, C. H. (2021). The impact of trophic and immunomodulatory factors on oligodendrocyte maturation: Potential treatments for encephalopathy of prematurity. *Glia*, *69*, 1311–1340. https://doi.org/10.1002/glia.23939

Vautier, F., Belachew, S., Chittajallu, R., & Gallo, V. (2004). Shaker-type potassium channel subunits differentially control oligodendrocyte progenitor proliferation. *Glia*, *48*, 337–345.

Wang, F., Ruppell, K. T., Zhou, S., Qu, Y., Gong, J., Shang, Y., Wu, J., Liu, X., Diao, W., Li, Y., & Xiang, Y. (2023). Gliotransmission and adenosine signaling promote axon regeneration. *Developmental Cell*, *58*, 660–676.e7. https://pubmed.ncbi.nlm.nih.gov/37028426/

Wei, W., Du, C., Lv, J., Zhao, G., Li, Z., Wu, Z., Haskó, G., & Xie, X. (2013). Blocking A2B adenosine receptor alleviates pathogenesis of experimental autoimmune encephalomyelitis via inhibition of IL-6 production and Th17 differentiation. *The Journal of Immunology*, *190*, 138–146. https://pubmed.ncbi.nlm.nih.gov/23225885/

Zhang, E., Tian, X., Li, R., Chen, C., Li, M., Ma, L., Wei, R., Zhou, Y., & Cui, Y. (2021). Dalfampridine in the treatment of multiple sclerosis: A meta-analysis of randomised controlled trials. *Orphanet Journal of Rare Diseases*, *16*, 87.

Zonouzi, M., Renzi, M., Farrant, M., & Cull-Candy, S. G. (2011). Bidirectional plasticity of calcium-permeable AMPA receptors in oligodendrocyte lineage cells. *Nature Neuroscience*, *14*, 1430–1438.

SUPPORTING INFORMATION

Additional supporting information can be found online in the Supporting Information section at the end of this article.